frontiers in Earth Science

ORIGINAL RESEARCH
published: 26 September 2017
doi: 10.3389/feart.2017.00075

A New Perspective on the Apparent Solubility of Dissolved Black Carbon

*Sasha Wagner†, Yan Ding and Rudolf Jaffé**

Department of Chemistry and Biochemistry, Southeast Environmental Research Center, Florida International University, North Miami, FL, United States

Black carbon (BC), pyrogenic organic matter generated from the incomplete combustion of biomass, is ubiquitous in the environment. The molecular structures which comprise the BC pool of compounds are defined by their condensed aromatic core structures polysubstituted with O-containing functionalities (e.g., carboxyl groups). Despite the apparent hydrophobicity of BC molecules, a considerable portion of BC is translocated from terrestrial to aquatic systems in the form of dissolved BC (DBC). However, the specific biogeochemical mechanisms which control the transfer of BC from the land to the water remain elusive. In the current study, the apparent solubility of DBC was inferred from octanol-water partition coefficients (K_{ow}) modeled for proposed DBC structures with varying degrees of polycondensation and polar functionality. Modeled K_{ow} values indicated that DBC molecules with small aromatic ring systems and high degrees of hydrophilic functionality may be truly solubilized in the aqueous phase. However, large and highly condensed DBC structures yielded high K_{ow} values, which suggested that a considerable portion of the DBC pool which has been quantified in aquatic environments is not truly dissolved. We hypothesized that other DOM components may act as mediators in the solubilization of condensed aromatic molecules and serve to increase the solubility of DBC via hydrophobic, intermolecular associations. This hypothesis was tested through controlled leaching experiments to determine whether the mobilization of DBC from particulate soils and chars became enhanced in the presence of DOM. However, we observed that characteristics inherent to each sample type had a greater influence than added DOM on the apparent solubility of DBC. In addition, the direct comparison of molecular marker (benzenepolycarboxylic acids) and ultrahigh resolution mass spectral data (FT-ICR/MS) on leachates obtained from the same set of soils and char did not show a clear overlap in DBC quantification or characterization between the two analytical methods. Correlations between FT-ICR/MS results and BPCA were not significant possibly due to differences in the methodological windows and/or small sample size. Our results were unable to provide evidence in support of proposed hydrophobic interactions between DOM and DBC, suggesting that other physical/chemical mechanisms play important roles in the dissolution of BC.

Keywords: Dissolved Black Carbon, octanol-water partition coefficient, K_{ow}, soil, charcoal, benzenepolycarboxylic acid method, apparent solubility, condensed aromatics

OPEN ACCESS

Edited by:
Cristina Santin, Swansea University, United Kingdom

Reviewed by:
William C. Hockaday, Baylor University, United States
Philippa Louise Ascough, Scottish Universities Environmental Research Centre, United Kingdom

****Correspondence:***
Rudolf Jaffé
jaffer@fiu.edu

†Present Address:
Sasha Wagner, Marine Sciences Department, Skidaway Institute of Oceanography, University of Georgia, Savannah, GA, United States

Specialty section:
This article was submitted to Biogeoscience, a section of the journal Frontiers in Earth Science

Received: *31 May 2017*
Accepted: *12 September 2017*
Published: *26 September 2017*

Citation:
Wagner S, Ding Y and Jaffé R (2017) A New Perspective on the Apparent Solubility of Dissolved Black Carbon. Front. Earth Sci. 5:75. doi: 10.3389/feart.2017.00075

INTRODUCTION

Black carbon (BC) is generated from the incomplete combustion of biomass and fossil fuel (Goldberg, 1985). The chemical composition of BC is heterogeneous (Masiello, 2004), ranging from mildly thermally altered biomolecules (Myers-Pigg et al., 2015) to condensed aromatic structures produced during high temperature combustion (Schneider et al., 2010). It is estimated that global production of BC from biomass burning is up to 383 Tg per year and most of the BC produced through fire is deposited on the landscape (Santín et al., 2015). The stability of BC which is incorporated into soils is highly variable, with residence times ranging from days to millennia (Bird et al., 2015). The ubiquity of fire and the refractory nature of condensed aromatics have resulted in the accumulation of BC in soils, where it comprises ∼14% of global soil C stores (Reisser et al., 2016). Despite the observed refractory nature of soil BC (Kuzyakov et al., 2014), the apparent solubilization and subsequent transport via rivers as DBC has been identified as a major loss process of BC from terrestrial environments (Dittmar et al., 2012; Jaffé et al., 2013; Stubbins et al., 2015). As such, it was estimated that DBC accounts for ∼10% of the total DOC flux exported annually by global rivers to the oceans (Jaffé et al., 2013). It seems clear that fluvial transfer of DBC to the ocean represents a key component of global C cycles (Santín et al., 2015). However, very little is known regarding the geochemical mechanisms which control the release of soil BC to inland waters as DBC.

Although, recent wildfire activity does not seem to have a significant effect on in-stream DBC (Ding et al., 2013; Güereña et al., 2015; Wagner et al., 2015a), this material is continually exported from fire-impacted watersheds for decades after a burn event (Dittmar et al., 2012). This suggests that the aging of BC in soils may be a prerequisite to its dissolution and export to aquatic systems as DBC. Soil BC structures undergo surface oxidation with increasing soil residence time (Cheng et al., 2006; Zimmerman, 2010), and it is thought that this type of oxidation enhances the mobilization of DBC from aged charcoal (Abiven et al., 2011). Although, the oxidation of BC has been shown to result in the formation of O-containing functional groups on condensed aromatic structures (Cheng et al., 2006; Zimmerman, 2010), it is unknown whether such diagenetic processing increases the polarity of BC molecules above a threshold where DBC molecules are truly solubilized in water.

This study refers to specifically BC and DBC as the polycondensed aromatics isolated from soils, chars, and natural waters and then oxidized to yield benzenepolycarboxylic acid (BPCA) products (Dittmar, 2008). The BPCA method, which chemically converts condensed aromatics to individual benzene rings substituted with three, four, five, and six carboxylic acid groups (B3CA, B4CA, B5CA, and B6CA, respectively), has been identified as a robust approach for measuring and characterizing BC in environmental matrices (Roth et al., 2012). To generate B6CA, the parent DBC structure must contain 5 or more non-linear fused aromatic rings (Ziolkowski et al., 2011), which equates to a structure containing a minimum of 20 carbon atoms. Since DBC collected from surface waters yields considerable amounts of B6CA (e.g., Ding et al., 2013; Wagner et al., 2015a), it can be inferred that larger DBC structures (>5 fused aromatic rings) are readily mobilized to the dissolved phase in natural systems. However, the stabilization of such large DBC molecules in the water column is not well understood as the hydrophobic, condensed aromatic core structures of these pyrogenic compounds would suggest they are largely insoluble in water.

The aqueous solubility of molecular structures can be inferred from the octanol-water partition coefficient (K_{ow}), which is experimentally defined as the ratio of a compound's concentration in octanol to its concentration in pure water (Schwarzenbach et al., 2003 and references therein). For compounds that cannot be isolated or do not have commercially-available standards, such as the molecules which comprise the DBC pool, K_{ow} is estimated using computational calculations based upon the atom/fragment contribution method which breaks down the proposed chemical structure into its fragment components and functional groups (Meylan and Howard, 1995). The K_{ow} is also a proxy for the DOC-water partition coefficient (Karickhoff, 1981; Seth et al., 1999; Schwarzenbach et al., 2003), where compounds with high K_{ow} values have greater affinities for organic matter (OM), including DOC in aqueous solution. The apparent solubilities of polyaromatic hydrocarbons (PAHs), which feature a condensed aromatic structure similar to DBC, are enhanced by DOM (Perminova et al., 1999; Durjava et al., 2007). Therefore, DOM may assist in the solubilization and stabilization of DBC molecules in the water column.

Since DOM is operationally-defined as organic matter which passes through a filter (pore size = 0.7 μm in the current study), the term "DBC" should include all physical forms of BC associated with the operationally-defined DOM pool (e.g., truly dissolved molecules, colloids, micelles, nanoparticles, etc.). Humic substances are proposed to exist as supramolecular assemblies of relatively small, heterogeneous molecules, which likely includes DBC, stabilized by weak hydrophobic interactions such as van der Waals forces, H-bonding, cation bridging, etc. (Piccolo, 2001; Simpson et al., 2002). In addition, DBC has been reported to preferentially associate with high molecular weight, humic-type DOM (Wagner and Jaffé, 2015), further supporting a potential DBC-DOM hydrophobic partitioning mechanism. The aromatic content of natural organic matter seems to play a key role in the binding of condensed aromatic compounds (Perminova et al., 1999), which suggests that conjugated aromatic π-systems may strengthen DBC-DOM relationships via specific electron donor-acceptor interactions (Keiluweit and Kleber, 2009). As such, we hypothesized that the apparent solubility of DBC (i.e., the amount of solubilized DBC, as defined by BC which passes through a 0.7 μm filter) may be facilitated or enhanced via macromolecular associations with components of natural DOM. In the current study, we have taken a three-pronged approach by combining computer modeling techniques, controlled leaching experiments, and ultrahigh resolution FT-ICR/MS analysis to test the effects of added DOM on the dissolution of DBC from soils and chars and to investigate the discrepancy between DBC molecular structure and its apparent solubility.

MATERIALS AND METHODS

Selection of Dissolved Black Carbon Molecular Formulae

The DBC molecules selected to be modeled in this study were chosen from existing literature reports. DOM from charcoal leachates had been previously characterized using Fourier transform ion cyclotron resonance mass spectrometry (FT-ICR/MS; Hockaday et al., 2007), an ultrahigh resolution analytical technique which allows for the assignment of individual molecular formulae to mass spectral peaks (Kujawinski, 2002; Sleighter and Hatcher, 2007; Dittmar and Paeng, 2009). Details regarding instrumental conditions and assignment of molecular formulas have been previously described by Hockaday et al. (2006, 2007). From the list of assigned molecular formulae identified for the charcoal leachate samples (**Table 1**; Hockaday et al., 2006), limitations for normalized double bond equivalents (DBE/C $\geq$ 0.7; Hockaday et al., 2006) and the aromaticity index (AI $\geq$ 0.67; Koch and Dittmar, 2006) were applied to specifically select molecular formulae with condensed aromatic ring structures. DBC molecular formulae which fit the following criteria were chosen for further consideration: (a) DBE/C $\geq$ 0.7, (b) AI $\geq$ 0.67, and (c) carbon number > 20 (strongly indicative of pyrogenic origin; Wagner et al., 2015b). Using this approach, a total of 32 formula combinations in the form of $C_mH_nO_{x1\sim x2}$ (where m, n, and x designate numbers of C, H, and O atoms, respectively) were selected to represent a range of DBC compounds (Table S1). From the list of 32 formulas, 12 molecular formulae, which covered the entire mass range, were chosen for the modeling of K_{ow} DBC values. The 12 selected DBC molecular formulae are summarized in **Table 1**. Since the K_{ow} of a DBC molecular structure was expected to be inversely correlated with the number of O-containing functionalities it contained, formulas with the smallest number of O atoms ($C_mH_nO_{x1}$) were chosen to represent the upper range of K_{ow} values and molecular formulas with the largest number of O atoms ($C_mH_nO_{x2}$) were chosen to represent the lower range of K_{ow} values for DBC formulae sharing the same number of C and H atoms (**Table 1** and Table S1).

TABLE 1 | Empirical DBC molecular formulae selected for K_{ow} modeling.

Formula	#C (m)	#H (n)	#O (×1)	#O (×2)	DBE/C	AI (min)	AI (max)
$C_{20}H_{12}O_{5\sim5}$	20	12	5	5	0.75	0.67	0.67
$C_{21}H_{12}O_{5\sim6}$	21	12	5	6	0.76	0.67	0.69
$C_{22}H_{12}O_{4\sim7}$	22	12	4	7	0.77	0.67	0.72
$C_{23}H_{14}O_{5\sim5}$	23	14	5	5	0.74	0.67	0.67
$C_{24}H_{14}O_{3\sim6}$	24	14	3	6	0.75	0.67	0.71
$C_{26}H_{16}O_{4\sim5}$	26	16	4	5	0.73	0.67	0.68
$C_{26}H_{14}O_{4\sim8}$	26	14	4	8	0.77	0.67	0.73
$C_{28}H_{18}O_{4\sim4}$	28	18	4	4	0.71	0.67	0.67
$C_{28}H_{14}O_{4\sim10}$	28	14	4	10	0.79	0.67	0.75
$C_{30}H_{18}O_{5\sim6}$	30	18	5	6	0.73	0.67	0.68
$C_{30}H_{14}O_{5\sim12}$	30	14	5	12	0.8	0.67	0.76
$C_{32}H_{14}O_{6\sim14}$	32	14	6	14	0.81	0.67	0.77

The formulae were originally identified in soil charcoal DOM by Hockaday et al. (2006).

Assembling Proposed Dissolved Black Carbon Molecular Structures

All possible arrangements for polyaromatic core structures containing 5–8 fused rings were drawn using Chem3D (Version Pro 12; CambridgeSoft Corporation). A selection of some of the proposed core structures and calculated H/C ratios are shown in Table S2. While the number of possible arrangements for small core structures (e.g., 5-ring systems) was limited, the number of possible arrangements for large core structures (e.g., 8-ring systems) was more extensive and it would have been prohibitively difficult to assess them all. Thus, core structures which exhibited the highest and lowest H/C ratios (the most linear and most condensed ring arrangements, respectively) were selected to model a range of possible K_{ow} values for proposed DBC structures with large aromatic ring systems. Although, condensed aromatic molecules with unsatisfied valences (radicals) can exist as part of DBC, radical-containing DBC structures were not considered for K_{ow} modeling.

DBC structures were assembled by first choosing an aromatic core structure from **Table 1**, then using the remaining numbers of C, H, and O atoms for the assignment of O-containing functional groups (e.g., −OH, −CHO, −COOH). Any remaining C and H atoms after O-assignments were incorporated into the structure as aliphatic side chains (e.g., $-CH_3$, $-CH_2-$). The effect of O-containing functional groups on increasing the K_{ow} of a condensed aromatic structure is in the order of −OH < −CHO < −COOH (Meylan and Howard, 1995). To estimate the highest K_{ow} values for $C_mH_nO_{x1}$ formulae, O-functionalities were added primarily as carboxyl groups. To estimate the lowest K_{ow} values for $C_mH_nO_{x2}$ formulae, O-functionalities were added primarily as hydroxyl groups. This approach allowed for the assessment of the widest possible range of modeled K_{ow} values for each DBC formula pair. Structural planarity enhances the partitioning of hydrophobic organic compounds to humic substances (Gauthier et al., 1987; Chin et al., 1997; Uhle et al., 1999). Since we hypothesize DBC molecules to participate in such hydrophobic interactions with DOM, we sought to maximize the structural planarity of proposed DBC structures in the current study. To minimize steric hindrance, which compromises the molecular planarity of DBC molecules, adjacent positioning of functional groups was avoided. Proposed DBC structures which exhibited the lowest molecular energy and the highest planarity were ultimately selected for K_{ow} modeling. The determination of proposed molecular structures for an exemplary pair of DBC formulae is detailed in the Supporting Information (Tables S2, S3; Figure S3).

Modeling K_{ow} for Proposed Dissolved Black Carbon Molecular Structures

The atom/fragment contribution method (Meylan and Howard, 1995) was used to estimate the K_{ow} of proposed DBC molecular structures. The modeling of K_{ow} values for DBC structures

was performed using the EPI Suite™-Estimation Program Interface program developed by the Environmental Protection Agency (EPA; USA; https://www.epa.gov/tsca-screening-tools/epi-suitetm-estimation-program-interface), which operates based upon the atom/fragment contribution method. Briefly, DBC molecular structures were disassembled into "fundamental fragments" consisting of isolated C atoms, H atoms, O atoms, and functional groups. The coefficient values of individual fragments were summed and correction factors were applied to obtain the K_{ow} value for DBC structures.

Collection and Characterization of Soil and Char Samples

Soil and char samples were obtained from diverse sources and locations to comprise a suite of naturally-occurring organic matter samples and reference materials which were expected to yield a gradient of OC content, BC content, and physical characteristics. Soils were collected from the natural environment in areas having a known history of biomass burning. Peat soil was obtained from the Florida Coastal Everglades (SRS2S; Florida, USA) in an area which undergoes prescribed burning and potentially receives additional pyrogenic inputs from burned sugarcane fields located upstream through canal inputs. Surface soil was collected from a historic charcoal blast furnace site (PA2S; Pennsylvania, USA) which known to contain high amounts of BC (Cheng et al., 2008). Surface soil collected from a forested area which burned during the High Park wildfire in June of 2012 (PNAS; Colorado, USA) represented a soil with relatively fresh pyrogenic inputs. Topsoil was collected from the Hubbard Brook Experimental Forest (HBRS; New Hampshire, USA) from an area which experienced a large wildfire during the 1920s and was therefore used as reference of soil containing aged charcoal. Char samples representing diverse biomass sources and charring conditions were also obtained. Charcoal standards generated from rice straw (RICEC) and chestnut wood (WOODC) were obtained from the University of Zurich (Switzerland). Formation conditions and characterization of these two chars are described in detail by Hammes et al. (2006). Wildfire-derived char was directly removed from a severely burned pine tree from the area of the High Park wildfire (PNAC; Colorado, USA). Although, PNAC was exposed to some degree of natural weathering and sunlight prior to collection, it had experienced no direct soil interaction. Pieces of charcoal were collected from the crater left by an uprooted tree (∼8 cm from ground surface) at the site of the 1920s wildfire in the Hubbard Brook Experimental Forest (HBRC; New Hampshire, USA). Since this area of the Hubbard Brook forest has experienced no direct wildfires since the 1920s, HBRC represented an aged char sample. Field-collected soils and chars were stored frozen at −20°C and charcoal standards were stored in the dark at room temperature until further processing. Frozen samples were subsequently thawed and air dried. Coarse particulates were removed by hand and samples were ground using a mortar and pestle and passed through a sieve (30 mesh; 600 μm pore size). Homogenized samples were then dried overnight at 60°C and stored in a desiccator until further use. The OC content of soils and chars was measured via elemental analysis-isotope ratio mass spectrometry using a NA 1,500 Elemental analyzer and a Delta Plus IRMS with a Conflo 2 Dilution interface. Mineral content was determined using the loss on ignition method as described by Hammes et al. (2006). Briefly, samples were dried at 105°C for 24 h, then ignited at 500°C for 4 h. The mineral content was calculated as the proportion of the mass remaining after ignition to the total mass of the sample prior to ignition.

Leaching Experiment and Analysis of Soil and Char Leachates

Dry soils and chars (0.4 g OC) were directly weighed into pre-combusted glass Erlenmeyer flasks and leached with three different aqueous phases (150 mL): deionized water (pH = 7), Pony Lake fulvic acid solution (PLFA; 5 mg-C L^{-1}; pH = 6), and Suwannee River humic acid solution (SRHA; 5 mg-C L^{-1}; pH = 6). PLFA and SRHA DOM standards were purchased from the International Humic Substances Society (IHSS; www.ihss.humicsubstances.org). Leachates were obtained in triplicate. Individual flasks containing deionized water, PLFA solution, and SRHA solution were included as controls for each leaching setup. Soil/Char suspensions and controls were capped and agitated on a shaker table (160 rpm) in the dark at 25°C for 72 h. The samples were subsequently filtered through pre-combusted 0.7 μm GF/F filters and rinsed with 110 mL deionized water, which brought final sample volumes to 260 mL. Filtered leachates and control solutions were stored at 4°C until further analysis.

DOC was measured using a Shimadzu TOC-V-CSH analyzer (Shimadzu Corporation, Tokyo, Japan). Ionic strength and pH were obtained with Accumet conductivity and pH probes (Fisher Scientific). Filtrates were acidified to pH 2 with concentrated HCl and DOM was isolated by solid phase extraction using the method outlined by Dittmar et al. (2008). Briefly, the Varian Bond Elut PPL cartridge (1 g) was first conditioned with Optima-grade MeOH and equilibrated with pH 2 MilliQ water. The acidified filtrate was then passed through the cartridge by gravity and the sorbent was subsequently rinsed with pH 2 MilliQ water to remove excess salts and subsequently dried under a stream of N_2. The DOM was then eluted with MeOH and stored in the dark at −20°C until DBC quantification.

Black Carbon Quantification and Characterization via the Benzenepolycarboxylic Acid (BPCA) Method

BC was quantified and characterized in all samples using the BPCA method (Dittmar, 2008; Ding et al., 2013; Wiedemeier et al., 2016). For leachate samples, where DOM was isolated via solid phase extraction, aliquots of the DOM-containing MeOH elute were transferred to 2 mL glass ampules and the MeOH evaporated under a stream of N_2 gas. Concentrated nitric acid (0.5 mL) was subsequently added to each ampule, which were then flame-sealed and heated to 160°C for 6 h in a programmable oven to oxidize the condensed aromatic DOM to BPCAs. After oxidation, the ampules were heated to 50°C in a sand bath and the HNO_3 was evaporated under a stream of N_2 gas.

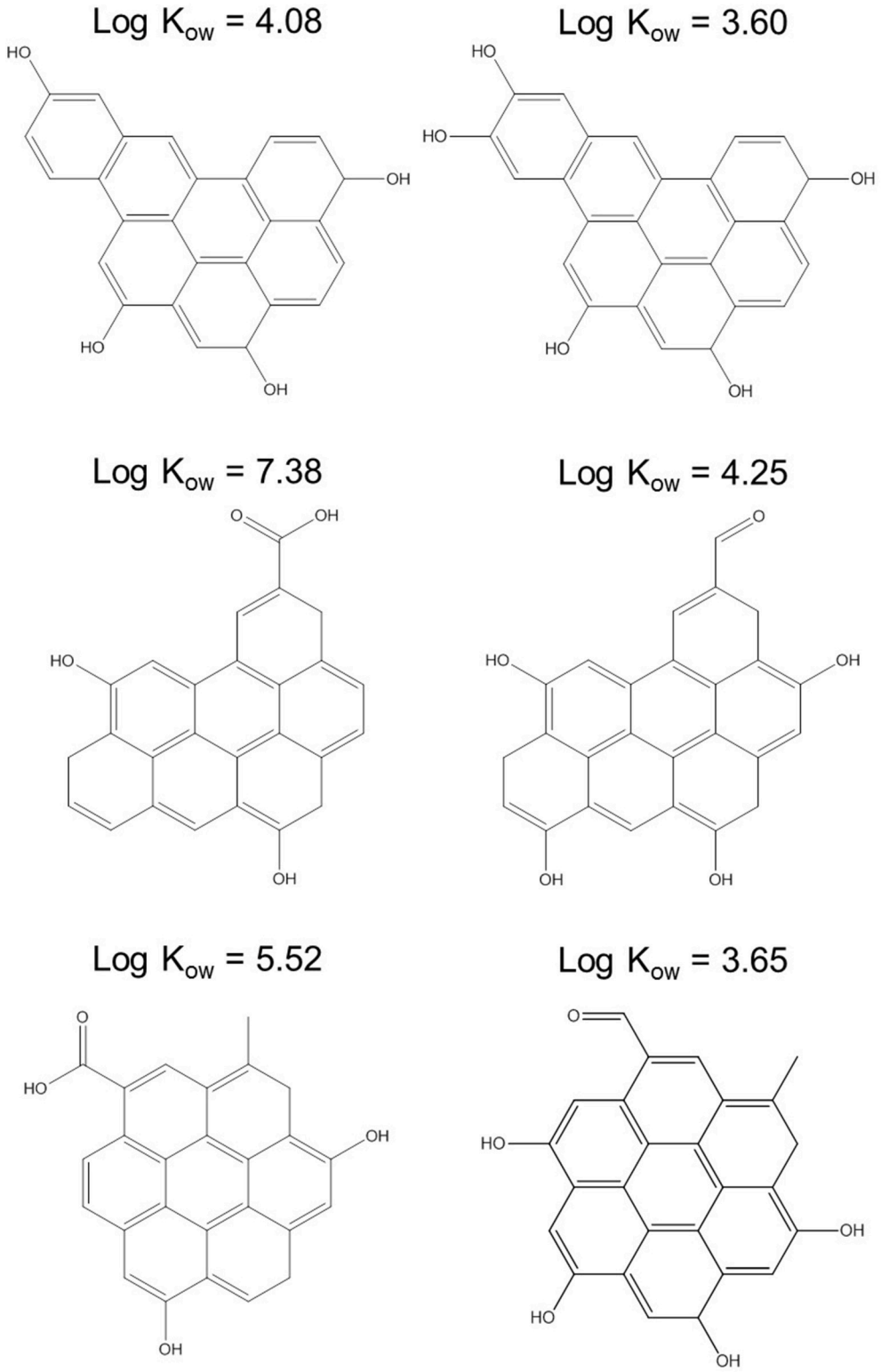

FIGURE 1 | A selection of proposed DBC molecular structures and modeled log K_{ow} values.

The residue containing BPCAs was dissolved in the mobile phase for analysis. High pressure liquid chromatography (HPLC) separation of BPCAs was performed using a Sunfire C18 reversed phase column (3.5 μm, 2.1 × 150 mm; Waters Corporation). A gradient elution method was employed with mobile phase A (4 mM tetrabutylammonium bromide, 50 mM sodium acetate, 10% MeOH) and mobile phase B (100% MeOH) as described in detail by Dittmar (2008). BPCA oxidation and analysis for each sample was carried out in triplicate (CV < 5%).

Procedures for measuring DBC were scaled up to accommodate the oxidation of larger amounts of organic material for the determination of BC in the particulate soil and char samples. Additional clean-up steps were also required for the BC analysis of solid samples in order to remove metals and other interfering compounds prior to BPCA analysis (Schneider et al., 2010, 2011). The particulate BPCA procedure has been described in detail by Wiedemeier et al. (2016). Briefly, dry sample (∼2 mg) was directly transferred to 20 mL glass ampules. Concentrated HNO_3 (2 mL) was added and ampules were immediately flame-sealed and oxidized under the conditions described above. After oxidation, contents of each ampule were filtered through a pre-rinsed filter (0.7 μm GF/F), passed over a cation exchange resin (Dowex 50 WX8 400) and the eluent freeze-dried. The BPCA-containing residue was then re-dissolved in a 1:1 solution of Milli-Q water and MeOH and passed through a C18 solid phase extraction cartridge (Supelco). The eluent was collected, freeze-dried and re-dissolved for a final time in the mobile phase for HPLC analysis as described above. BPCA determinations for soils and chars were carried out in triplicate.

Fourier Transform Ion Cyclotron Resonance Mass Spectral (FT-ICR/MS) Analysis of Water-Leached Soils and Chars

Methanol DOM extracts for water-leached soils and chars were diluted to DOC concentrations of ∼20 mg-C L^{-1} in MeOH and Milli-Q water (1:1 v/v) and passed through a Teflon filter (0.2 μm) prior to electrospray ionization. Mass spectral analyses were carried out at the University of Oldenburg (Germany) on a Bruker Solarix 15 Tesla FT-ICR/MS instrument in negative ion mode, with 500 scans collected per sample. A reference mass list was used to calibrate each spectrum. The data were filtered to remove peaks that only appeared in one sample and those with low signal/noise ratio (<3). Formulas containing C, H, O, N, S, and P were assigned to mass spectral peaks, then filtered to remove unlikely DOM molecular combinations as described by Koch et al. (2007). The modified aromaticity index ($AI_{mod} \geq 0.67$) outlined by Koch and Dittmar (2006) was used to unambiguously categorize formulae with condensed aromatic structures, here referred to as DBC.

RESULTS

Modeled K_{ow} Values for Proposed Dissolved Black Carbon Structures

In total, 90 molecular structures were derived from DBC formulae (**Table 1**) to constrain upper ($C_mH_nO_{x1}$; $n = 42$) and lower ($C_mH_nO_{x2}$; $n = 48$) ranges in K_{ow} for compounds with five to eight fused aromatic rings. Exemplary molecular structures and modeled log K_{ow} values for a selection of DBC formulae used in this exercise are shown in **Figure 1**. The modeled DBC structures in the current study are similar to those previously derived from molecular formulas assigned to FT-ICR mass spectral peaks (Kramer et al., 2004; Dittmar and Koch, 2006). The number of C+H-O atoms was calculated for each of the selected DBC molecular formulae in **Table 1** (C+H-O ranged from 27 to 44) and regressed against the log K_{ow} values determined using the atom-fragment contribution method for O-depleted ($C_mH_nO_{x1}$) and O-enriched ($C_mH_nO_{x2}$) molecular structures. Linear correlations and associated regression equations between log K_{ow} and number of C+H-O atoms are shown in **Figure 2**. Log K_{ow} values estimated for O-depleted DBC formulae ranged from 3.51 to 8.04 and averaged 5.74 ± 1.26. Log K_{ow} values estimated for O-enriched DBC formulae ranged from 1.48 to 6.67 and averaged 3.97 ± 1.35.

Analysis of Particulate Soils, Particulate Chars, and Leachate Samples

The amount of DOC in each leachate solution (from deionized water, SRHA, and PLFA treatments) was corrected for the contribution of DOC from PLFA and SRHA (0.50 ± 0.05 and 0.47 ± 0.07 mg-C, respectively) and normalized to the amount of OC in the particulate sample. Leachate DOC ranged from 0.98 to 22.0 mg g-OC^{-1} with a median DOC yield of 3.74 mg g-OC^{-1}. The amount of DBC in each leachate solution was also corrected for the contribution of DBC from PLFA and SRHA (quantified via the BPCA method in our lab as contributing 0.011 ± 0.003 and 0.043 ± 0.005 mg-C, respectively)

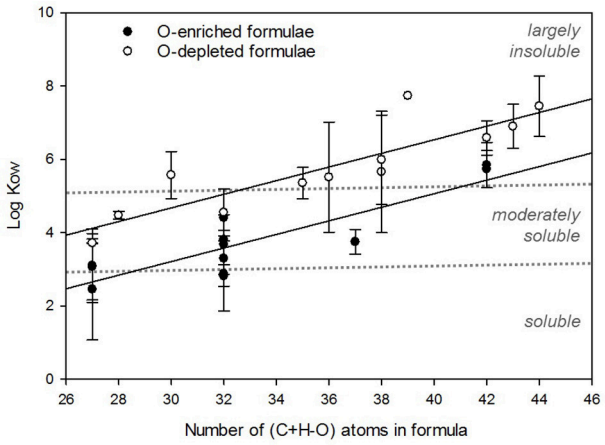

FIGURE 2 | Linear correlations between the log K_{ow} and C+H–O number for 90 proposed DBC structures. Data points were binned according to their C+H–O number. O-depleted formulae ($C_mH_nO_{x1}$) were used to calculate the high log K_{ow} regression (y = 0.186x – 0.907; $R^2 = 0.77$) and O-enriched formulae (all $C_mH_nO_{x2}$) were used to calculate the low log K_{ow} regression (y = 0.185x – 2.350; $R^2 = 0.76$). Each point represents the binned mean and error bars represent 1 SD.

and normalized to the amount of OC in the particulate sample. Leachate DBC ranged from 0.04 to 2.58 mg g-OC^{-1} with a median DBC yield of 0.26 mg g-OC^{-1}. Deionized water blanks contained negligible amounts of DOC and DBC. The pH of leachate solutions ranged from 4.3 to 8.4 and conductivity spanned a range of 6–417 μs cm^{-1}. A complete list of data for the leachate solutions is listed in **Table 2**. Error associated with experimental replicates (median and average CV across all experimental conditions were 22 and 32%, respectively) was greater than the error associated with analytical replicates (CV < 5%). Therefore, analytical error was assumed to be negligible when calculating net DBC values. Standard deviations listed in **Table 2** are instead representative of the larger error associated with experimental replicates. A detailed description on error propagation in the current study can be found in the Supporting Information.

The OC content of the soils and chars ranged from 7.6 to 65.8 g kg^{-1} with a median of 59.1 g kg^{-1}. Mineral content, calculated as the mass of material remaining after loss on ignition, ranged from 36 to 837 g kg^{-1} with a median value of 193 g kg^{-1}. The BC content of the particulate samples spanned a range of 28–357 g kg-OC^{-1} with a median value of 272 g kg-OC^{-1}. A complete list of data for particulate soil and char samples is listed in **Table 3**.

Fourier Transform Ion Cyclotron Resonance Mass Spectral (FT-ICR/MS) Assessment of Water-Leached Soils and Chars

Ultra high resolution mass spectral analysis yielded more than 5,000 mass peaks per leachate sample. On average, water-leached soils and chars yielded 6,999 ± 1,271 mass peaks, to which an average of 4,874 ± 1,049 molecular formulas were assigned. The number of assigned molecular formulas which represented condensed aromatic structures (DBC; $AI_{mod} \geq 0.67$) containing only C, H, and O atoms ranged from 339 to 787. Mean-weighted average values for molecular weight (m/z) and number of C atoms per formula (#C) ranged from 283 to 355 and from 15.8 to 18.9, respectively. The linear regression between C+H-O and log K_{ow} established in **Figure 2** and described in section Modeled K_{ow} Values for Proposed Dissolved Black Carbon Structures was used to estimate log K_{ow} values for DBC formulas identified in the soil and char leachates. Most DBC formulas had an estimated log K_{ow} value < 3 (323 ± 45). Fewer DBC formulas had an estimated log K_{ow} between 3 and 5 (212 ± 77). A small number of DBC formulas had estimated log K_{ow} values > 5 (32 ± 28). Results of FT-ICR/MS analysis for individual leachate samples are listed in **Table 4**.

TABLE 2 | Experimental data for the DOM leached from soils and chars with deionized water, PLFA, and SRHA.

Sample	Treatment	DOC (g kg-OC^{-1})	DBC (g kg-OC^{-1})	pH	Conductivity (us cm^{-1})
SRS2 Soil	Water	2.44 ± 0.06	0.18 ± 0.09	8.33 ± 0.06	131 ± 1
SRS2 Soil	PLFA	2.26 ± 0.17	0.17 ± 0.04	8.30 ± 0.05	132 ± 2
SRS2 Soil	SRHA	1.92 ± 0.17	0.13 ± 0.02	8.36 ± 0.03	134 ± 2
PA2 Soil	Water	1.22 ± 0.09	0.22 ± 0.08	6.12 ± 0.04	6 ± 0
PA2 Soil	PLFA	0.98 ± 0.15	0.27 ± 0.07	5.90 ± 0.11	7 ± 1
PA2 Soil	SRHA	0.98 ± 0.20	0.26 ± 0.11	5.88 ± 0.09	6 ± 0
PNA Soil	Water	5.44 ± 0.06	0.67 ± 0.08	8.08 ± 0.04	89 ± 1
PNA Soil	PLFA	6.41 ± 2.58	0.68 ± 0.09	8.06 ± 0.05	88 ± 1
PNA Soil	SRHA	4.45 ± 0.31	0.65 ± 0.09	8.08 ± 0.06	87 ± 4
HBR Soil	Water	7.87 ± 0.18	0.24 ± 0.09	4.33 ± 0.02	21 ± 0
HBR Soil	PLFA	7.08 ± 0.53	0.24 ± 0.04	4.37 ± 0.06	22 ± 1
HBR Soil	SRHA	7.50 ± 0.23	0.25 ± 0.05	4.30 ± 0.03	23 ± 0
RICE Char	Water	21.97 ± 1.87	2.15 ± 0.12	8.11 ± 0.01	397 ± 2
RICE Char	PLFA	21.54 ± 0.70	2.06 ± 0.08	8.09 ± 0.04	402 ± 9
RICE Char	SRHA	21.97 ± 0.24	1.81 ± 0.31	8.02 ± 0.05	417 ± 9
WOOD Char	Water	3.49 ± 0.22	0.04 ± 0.00	8.01 ± 0.03	92 ± 4
WOOD Char	PLFA	2.86 ± 0.57	0.07 ± 0.01	8.07 ± 0.08	90 ± 5
WOOD Char	SRHA	2.86 ± 0.18	−0.02 ± 0.03	5.87 ± 1.86	37 ± 47
PNA Char	Water	2.57 ± 0.04	0.26 ± 0.18	7.49 ± 0.13	49 ± 0
PNA Char	PLFA	2.22 ± 0.17	0.29 ± 0.14	7.51 ± 0.08	48 ± 1
PNA Char	SRHA	2.24 ± 0.24	0.31 ± 0.15	7.57 ± 0.08	46 ± 1
HBR Char	Water	4.18 ± 0.18	0.27 ± 0.03	4.79 ± 0.27	12 ± 1
HBR Char	PLFA	3.99 ± 0.13	0.24 ± 0.07	4.35 ± 0.01	17 ± 0
HBR Char	SRHA	4.24 ± 0.20	0.22 ± 0.07	4.34 ± 0.01	17 ± 0

DOC and DBC values have been corrected for the inherent amount of DOC and DBC in PLFA or SRHA and are normalized by the mass of OC in the source soil or char. Conductivity and pH measurements were taken after the leachates were rinsed and diluted. All measurements were obtained in triplicate (mean ± 1 SD).

TABLE 3 | Characterization of soil and char samples.

Sample	Description	Sample ID	OC (g kg^{-1})	Mineral Content (g kg^{-1})	BC (g kg-OC^{-1})
SRS2 Soil	Everglades peat soil	SRS2S	509	345 ± 14	28 ± 8
PA2 Soil	Soil from historic charcoal furnace site	PA2S	570	342 ± 4	357 ± 12
PNA Soil	Alpine forest soil from area of recent wildfire	PNAS	76	837 ± 20	288 ± 120
HBR Soil	Temperate forest soil from area of historic wildfire	HBRS	494	113 ± 6	37 ± 2
RICE Char	Generated from rice straw (Hammes et al., 2006)	RICEC	632	193 ± 2	271 ± 4
WOOD Char	Generated from chestnut wood (Hammes et al., 2006)	WOODC	658	ND	274 ± 5
PNA Char	Charred pine tree burned in recent wildfire	PNAC	620	46 ± 3	259 ± 5
HBR Char	Derived from historic wildfire (wood type unknown)	HBRC	613	36 ± 13	295 ± 19

Mineral content was estimated by loss on ignition. ND denotes values below the detection limit.

TABLE 4 | FT-ICR mass spectral data for soils and chars leached with deionized water.

Sample	# mass peaks	# assigned formulas	# DBC formulas	m/z (w.a.)	#C (w.a.)	C+H-O (w.a.)	log K_{ow} (w.a.)	# formulas log K_{ow} <3	# formulas log K_{ow} 3–5	# formulas log K_{ow} >5
SRS2 Soil	7,907	6,021	467	301	15.8	18.1	1.72	310	149	8
PA2 Soil	8,517	5,942	787	355	18.9	21.3	2.33	380	326	78
PNA Soil	8,292	6,037	607	307	16.2	18.5	1.81	342	234	29
HBR Soil	6,180	4,169	563	330	16.6	17.9	1.70	341	212	8
RICE Char	6,069	4,126	575	299	16.3	20.1	2.10	285	227	61
WOOD Char	5,883	3,758	504	300	14.9	15.7	1.28	317	164	21
PNA Char	5,272	3,676	339	283	14.6	16.6	1.46	243	93	1
HBR Char	7,872	5,262	728	348	17.9	19.8	2.04	371	298	56

Mean-weighted average (w.a.) values and the number of formulas with log K_{ow} values <3, 3–5, and >5 are calculated from DBC formulae containing only C, H, and O.

DISCUSSION

Expected Solubility of Proposed Dissolved Black Carbon Structures Based Upon Modeled K_{ow} Values

The hydrophobic character and aqueous solubility of DBC cannot be experimentally determined since standard compounds which accurately represent the DBC pool do not exist. Instead, we gained insight into the solubility properties of DBC molecular structures from modeled K_{ow} coefficients (typically expressed as log K_{ow}) which were estimated using the atom/fragment contribution method (Meylan and Howard, 1995). As expected, DBC molecular structures with more O-containing functional groups exhibited, on average, significantly lower log K_{ow} values ($p < 0.05$), which suggests that more oxidized DBC molecules would have enhanced solubility in water. Significant, positive correlations were found between log K_{ow} and the number of C+H–O atoms ($p < 0.001$; **Figure 2**). The contribution of aromatic C fragments (e.g., = CH−) to a molecular structure increases its log K_{ow}, whereas the addition of O-containing functional groups (e.g., −OH, −COOH) decreases its log K_{ow} (Meylan and Howard, 1995; Schwarzenbach et al., 2003), therefore the positive relationship between C+H-O and log K_{ow} was expected. Log K_{ow} was also significantly positively correlated with the number of C+H atoms ($p < 0.001$; Figure S1) the number of fused aromatic rings in the DBC core structure ($p < 0.001$; Figure S2). Condensed aromatic structures with log K_{ow} values < 3 are quite soluble in water, with concentrations >1 mg L^{-1} (Tobiszewski and Namiesnik, 2012). Considering this conventional threshold for solubility assessment, it seems that some DBC structures may exist in a truly dissolved form (**Figure 2**). However, only 14% of the 90 proposed DBC structure are considered dissolved (log K_{ow} < 3), the rest fell within moderately soluble (3 < log K_{ow} < 5, 40%) and largely insoluble (log K_{ow} > 5, 46%) ranges. The majority of modeled log K_{ow} values derived from proposed DBC structures are above 3, indicating that many of the condensed aromatic structures which we have selected to represent the DBC pool have solubility limitations in water.

The log K_{ow} is inversely related to the aqueous solubility of hydrophobic organic compounds (Schwarzenbach et al., 2003 and references therein), such as polyaromatic hydrocarbons (PAHs), which share similar condensed aromatic structures as molecules within the DBC pool. Since PAHs are environmental pollutants, they have been well-characterized with regards to their solubility in water. PAHs containing 20 or more C atoms with log K_{ow} values > 5 are largely insoluble in water (corresponding to a concentration of ∼0.001 mg-C L^{-1} at 25°C; Tobiszewski and Namiesnik, 2012). From the apparent insolubility of large PAHs, we would expect DBC concentrations to be equally low in natural waters due to the structural similarities between DBC molecules and PAHs. DBC concentrations in natural waters often exceed 1 mg-C L^{-1} (Jaffé et al., 2013) and are enriched in B6CA (Ding et al., 2013, 2014; Wagner et al., 2015a). Taken together, the data yielded from BPCAs suggest that large (>20 C atoms) DBC molecules exist

and are somehow stabilized within the water column. However, this observation is at odds with K_{ow} modeling of DBC molecular structures derived from assigned molecular formulae (**Figure 2**).

Composition of Dissolved Black Carbon Leached from Soils and Chars

We carried out a controlled leaching experiment to investigate the discrepancy between the expected solubility of DBC (based upon above-described K_{ow} estimations from FT-ICR/MS formula assignments) and the quantity/quality of DBC measured in aquatic systems using the BPCA method. The composition of DBC, described by the relative abundance of individual BPCA molecular markers, in leachates extracted from soils and chars with deionized water was quite variable (**Figure 3A**). The relative abundance of BPCAs has been used as a proxy for BC condensed aromaticity, and greater proportions of B5CA and B6CA are indicative of more highly condensed aromatic BC (Schneider et al., 2010; Abiven et al., 2011). Molecular markers B5CA and B6CA were abundant in all leachate samples, comprising ∼20–50% of total BPCAs (**Figure 3A**). DBC leached from the soils was generally more enriched in B5CA and B6CA compared to DBC leached from the fresh chars, with the exception of PNAS. PNAS is a soil sample that received fresh charcoal inputs from a recent wildfire. Therefore, it was not surprising to find that the BPCA composition of PNAS resembled that of the fresh char leachates (WOODC, RICEC, PNAC; **Figure 3A**). HBRC, an aged char, leached greater proportions of B5CA and B6CA compared to the freshly-produced chars (**Figure 3A**). Similar findings have been previously reported in the literature (Abiven et al., 2011). Soil samples which have received historic inputs of BC (SRS2S, PA2S, HBRS) leached DBC with BPCA compositions similar to that of aged char. Over time, BC is presumably degraded and oxidized via biotic and abiotic processes (Cheng et al., 2006; Zimmerman, 2010) and it is proposed that the increase in polar functionality enhances the dissolution of larger DBC structures (those which generate greater proportions of B5CA and B6CA upon oxidation) from aged charcoal (Abiven et al., 2011). However, the modeling of log K_{ow} values for proposed DBC structures indicated that such oxidation processes do not sufficiently increase molecular polarity for the true solubilization of highly condensed DBC compounds in water. Therefore, other physico-chemical processes were considered to explain this phenomenon.

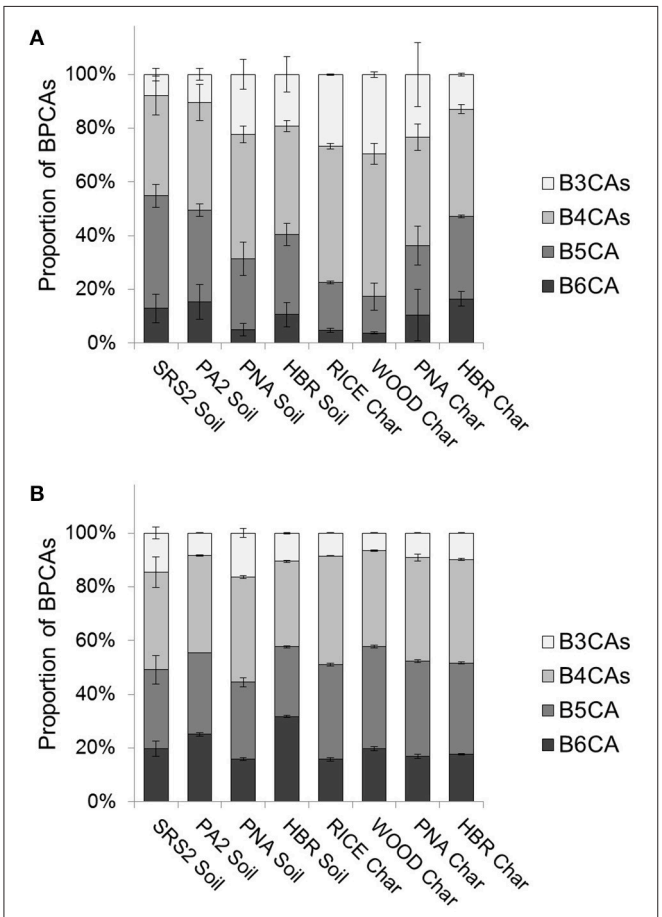

FIGURE 3 | Relative distributions of BPCAs for **(A)** DBC in water leachates and **(B)** BC in particulate soils and chars (error bars = 1 SD).

Effects of Dissolved Organic Matter on the Apparent Solubility of Dissolved Black Carbon

The DOM pool is operationally-defined by what passes through a filter (0.7 μm pore size in the current study), and therefore represents both truly dissolved compounds and macromolecular DOM structures (e.g., microparticulates, colloids, micelles, and molecular assemblies; Azam and Malfatti, 2007). In light of supramolecular theory, where humic substances are considered to be aggregates of smaller heterogeneous compounds held together by weak intermolecular forces (Piccolo, 2001; Simpson et al., 2002; Sutton and Sposito, 2005), it is hypothesized that the stabilization of DBC may result from hydrophobic interactions between condensed aromatic structures and other DOM components. Hydrophobic DOM aggregates in water as a result of entropy-driven associations to minimize contact with highly polar water molecules (Kleber and Johnson, 2010). Therefore, molecular interactions between highly condensed DBC compounds and DOM are likely to be more energetically-favorable than interactions between highly condensed DBC compounds and water. Supramolecular interactions have been shown to occur between high molecular weight PAHs and humic substances (Perminova et al., 1999) which enhances the apparent solubility of PAHs in solution (Chin et al., 1997; Mitra and Dickhut, 1999; Durjava et al., 2007). Considering the shared structural features between DBC and PAHs, DOM may facilitate the translocation of BC to surface waters via similar mechanisms. The proposed interactive relationship between DBC and other components of DOM is further supported by the global correlation observed between DBC and DOC in rivers (Jaffé et al., 2013).

The log K_{ow} has been used as a proxy for the partitioning of PAHs between the aqueous phase and natural organic matter (Karickhoff, 1981; Kopinke et al., 2002; Schwarzenbach et al., 2003). Therefore, highly polycondensed aromatic DBC compounds with modeled log K_{ow} values > 5 should have similarly high affinities for DOC. As such, we expected the leaching experiment to show enhanced solubilization of DBC from soils and chars in the presence of DOM compared with leaching with just deionized water alone. Commercially-available DOM standards, PLFA and SRHA, were selected to test the apparent solubility of DBC from soils and chars because they represent two distinct sources of natural DOM which exhibit different molecular characteristics. PLFA is sourced from an Antarctic lake, and contains DOM which is of predominantly autochthonous/microbial origin. SRHA is sourced from a blackwater river fed by peat swamps, and contains DOM of primarily terrigenous origin. We chose PLFA and SRHA for our controlled leaching experiments to determine whether the apparent solubility of DBC was at all affected by the molecular composition of the added DOM. The molecular structure of PLFA is primarily aliphatic with limited regions of aromatic functionality (Thorn et al., 1989), however, condensed aromatics have been shown to strongly interaction with fulvic acids in solution (Lu et al., 2013). As such, the apparent solubility of DBC was expected to increase when soils and chars were leached in the presence of PLFA. Since SRHA exhibits greater degrees of aromaticity than PLFA (Thorn et al., 1989), the apparent solubility of DBC was expected to be the greatest when soils and chars were leached in the presence of SRHA due to favorable interactions between the aromatic π-systems of fused ring structures and humic acids (Keiluweit and Kleber, 2009). The experimental data for soils and chars leached with water, PLFA, and SRHA are detailed in **Table 2**. Although enhanced mobilization of DBC was expected in the presence of PLFA and SRHA, this effect was not observed. The results of a two-way ANOVA showed that the effect of added DOM was not significant ($p = 0.17$), but the effect of sample type was significant ($p < 0.001$) for the net amount of DBC leached from soils and chars (**Figure 4**). This finding suggested that other factors, such as the characteristics of the soils and chars themselves, had a greater influence over the translocation of DBC to the dissolved phase than the proposed hydrophobic interactions with added DOM.

Supramolecular associations among organic matter components are complex and the specific mechanisms driving their relationships are not well-understood (Sutton and Sposito, 2005). Under the described experimental conditions, added humic and fulvic acid DOM did not have a significant effect on the net amount of DBC leached from soils and char (**Figure 4**; **Table 2**). The Supporting Information contains a detailed description of how errors were propagated for DBC values in **Figure 4**. There are several possible reasons for this observation: First, a considerable amount of DOC was generated from the soil and char samples themselves (2–20 mg-C L^{-1}; **Table 2**), and DBC may have been stabilized via thermodynamically favorable associations with existing soil DOM components. Interactions between BC and specific soil constituents have been demonstrated on the microscopic scale

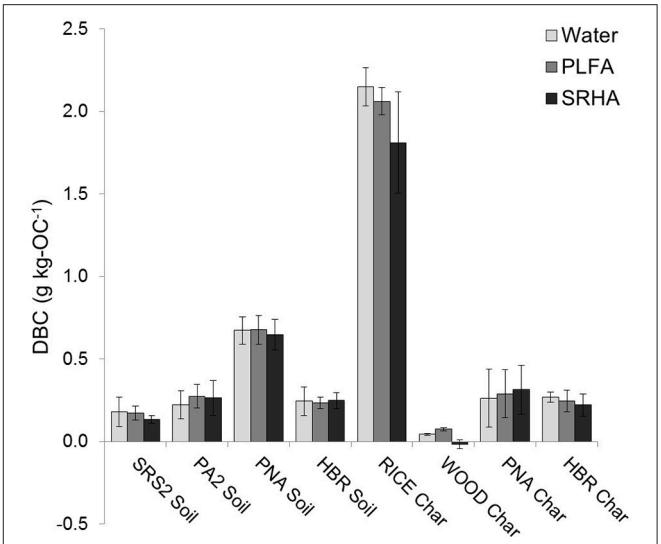

FIGURE 4 | Net DBC leached from soils and chars with water, PLFA, and SRHA (error bars = 1 SD).

(Lehmann et al., 2008; Kuo et al., 2013) and these existing associations could have minimized the potential effects of added DOM on DBC dissolution. Second, the concentrations of DOC generated directly from the soils and chars exceeded the concentrations of added PLFA and SRHA. DOC contributions from PLFA and SRHA were between 5 and 50% of final leachate DOC concentrations. Therefore, it is conceivable that the concentration of added DOM (5 mg-C L^{-1}) was too low to have a significant effect on the solubility of DBC. Third, in-lab experimental conditions are likely not an accurate reflection of leaching processes which occur in the natural environment. Batch experiments, in which the native aggregation of organic material and mineral components is destroyed and dry particulates are resuspended in solution, do not necessarily mimic the typical environmental conditions under which DOM is mobilized to surface waters (Kaiser et al., 2015). Finally, hydrophobic interactions may play more of a secondary role in the apparent solubility of DBC. Hydrophobic π-bond interactions are indeed the dominant interactive forces which mediate interactions for aromatic compounds lacking ionizable functional groups (e.g., PAHs; Keiluweit and Kleber, 2009). However, DBC structures are highly polysubstituted with polar, O-containing functionalities (Kramer et al., 2004; Wagner et al., 2015b), which may govern the interactions of these condensed aromatics with organic matter components by participating in other types of intermolecular forces, such as H-bonding, cation bridging, and chelation. If this is the case, then π-bond interactions would play more of an assistive role in the favorable interaction of DBC components to environmental sorbents (Keiluweit and Kleber, 2009). Chelation has been shown to distinctly affect DOM components differently based on their molecular character (Yamashita and Jaffé, 2008). Therefore, chelation processes could be an equally important driver of DBC molecular associations. The involvement of metals in the formation of inner-sphere complexes between

polar substituents, such as carboxylic groups, in DBC and between DBC and DOM, may indeed play a considerable, yet undetermined, role in DBC mobilization.

Comparing the Quantity and Quality of Dissolved Black Carbon Leached from Different Soils and Chars

This study was unable to provide experimental evidence to support the hypothesis that hydrophobic interactions with added DOM enhances the apparent dissolution of DBC. However, the significant variation in net amount DBC leached from a suite of soils and chars (**Figure 4**) suggested that physico-chemical factors other than associations between DBC and added DOM may drive the translocation of BC from soils and chars to the dissolved phase. HBRC leached more DBC than WOODC and PNAC which provides further support for the enhanced solubility of condensed aromatics in aged charcoal, relative to fresh charcoal, due to the increased degree of BC oxidation (Abiven et al., 2011). The RICEC sample leached, by far, the most DBC of all samples in the current study (**Figure 4**). Interestingly, the mineral content of RICEC was also high, ∼5 times greater than the mineral content of the wood chars (**Table 3**). Aromatic compounds, including BC, have been shown to preferentially interact with and sorb to mineral surfaces in soils (Brodowski et al., 2005; Kothawala et al., 2012) which suggests that mineral content may be an important control in the mobilization of DBC. However, no significant correlation was observed between mineral content of source soils and chars and net amount of DBC leached ($R^2 = 0.03$; $p = 0.66$; $n = 24$). Alternatively, charcoal generated from herbaceous-type biomass, such as RICEC, exhibits greater carboxyl functionality compared to wood-derived charcoal (Knicker et al., 1996), which may have contributed to the enhanced dissolution of DBC from RICEC.

The BC content of soil and char samples in this study varied considerably (**Table 3**), likely owing to diverse sources of biomass, combustion conditions, and compositions of the pyrogenic material (Masiello, 2004). Solid samples which were more enriched in BC did not necessarily yield greater amounts of DBC, as a significant correlation between BC content and net DBC leached was not observed ($R^2 = 0.04$; $p = 0.65$; $n = 24$). This finding suggests that measured amounts of BC in soils may not be indicative of expected DBC concentrations in soil pore water or inland waters which drain the local landscape. Since the leaching experiments were not buffered, the water-soluble components of soils and chars controlled the pH and ionic strength of their respective leachates (**Table 2**). Solution pH and ionic strength affect the conformation and macromolecular interactions of DOM (Kalbitz et al., 2000). However, leachate pH values were not found to be significantly correlated with amounts of leached DBC ($R^2 = 0.08$; $p = 0.17$; $n = 24$). Although, a significant linear correlation between conductivity and net amount of DBC released was observed ($R^2 = 0.80$; $p < 0.005$; $n = 24$), this relationship was diminished when the high conductivity values for RICEC were removed from the correlation ($R^2 = 0.00$; $p = 0.87$; $n = 21$). Similarly, a significant linear correlation between DBC and DOC was observed for all samples ($R^2 = 0.90$; $p < 0.001$; $n = 24$). However, this relationship was driven by the high amounts of DBC and DOC leached from RICEC, and the significance was diminished when RICEC was removed from the correlation ($R^2 = 0.00$; $p = 0.94$; $n = 21$). While potential effects of ionic strength and pH on the mobilization of DBC are indeed possible, the results presented here were inconclusive based upon the small set of samples in the current study.

To assess how the BPCA composition of mobilized DBC may be related its source, BC was characterized in the particulate soil and char samples (**Figure 3B**). The quality of BC across the entire sample set was generally similar, with B5CA and B6CA comprising ∼50% of total BPCAs. The degree of aromatic condensation for BC produced during wildfires is diverse, owing primarily to different biomass sources and combustion conditions (McBeath et al., 2013; Schneider et al., 2013). Therefore, the use of BPCA ratios as the sole proxy for DBC source is speculative since we still have a very poor understanding of the biogeochemical factors which influence BPCA composition during BC formation, mobilization, and degradation in the environment. However, we observed that leached DBC was consistently depleted in B5CA and B6CA relative to BC in their respective source soils and chars (**Figure 3**). This discrepancy suggests that the soluble portion of BC is indeed more enriched in DBC with smaller condensed aromatic ring systems than its particulate source. Results from the modeling of log K_{ow} for DBC structures, which predicts the enhanced solubility of condensed aromatic compounds with <5 fused rings, is in agreement with the observed preferential dissolution of less condensed DBC. However, BPCA compositions indicate that DBC leached from soils and chars also contained highly condensed aromatic structures (**Figure 3A**).

Contrasting the Quantification of DBC with Mass Spectral Data for Water-Leached Soils and Chars

To further probe the observed disconnect between DBC molecular markers and mass spectral composition, we applied the relationship between C+H-O and log K_{ow} (section Expected Solubility of Proposed Dissolved Black Carbon Structures Based upon Modeled K_{ow} Values) to estimate log K_{ow} values for DBC formulas identified by FT-ICR/MS in the current suite of soil and char leachates. Log K_{ow} values were estimated by averaging the log K_{ow} values obtained from both the O-depleted and O-enriched regression equations (**Figure 2**). A summary of the mass spectral data, including weighted-average values for C+H-O and estimated log K_{ow}, for water-leached soils and chars is listed in **Table 4**. The number of condensed aromatic molecular formulae varied among the sample set, with PA2S yielding the highest number of DBC peaks (787; **Table 4**). To visualize the mass spectral composition of DBC identified in PA2S, the condensed aromatic formulae were displayed in Van Krevelen space, where molecular formulas are plotted according to their H/C and O/C ratios (**Figure 5**). Modeled log K_{ow} values for DBC formulae generally increase with decreasing O/C ratio, which is in agreement with the hypothesis that the apparent solubility of DBC is enhanced by oxidation of condensed aromatic structures

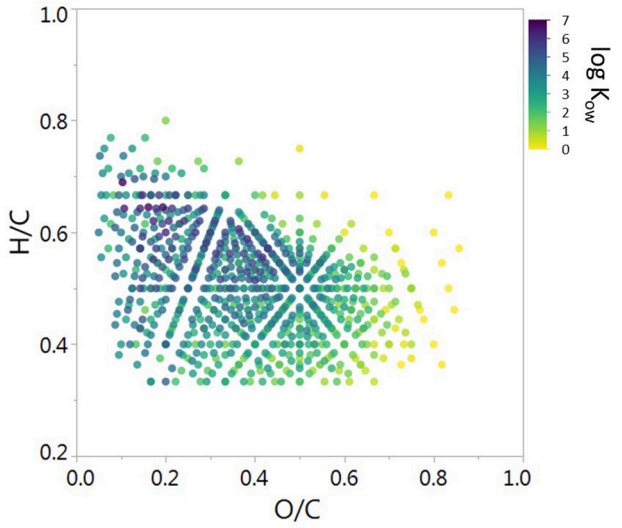

FIGURE 5 | Van Krevelen diagram of assigned DBC molecular formulae in the water leachate of PA2 Soil. Points are colored according to the estimated K_{ow} calculated from C+H-O regressions.

(Abiven et al., 2011). The Van Kevelen distribution also indicates that a large portion of DBC molecular formulae are quite soluble in water (log K_{ow} < 3; **Figure 5**). Line plots showing the distribution of C+H-O and estimated log K_{ow} for all soil and charcoal leachates are shown in **Figure 6**. Samples HBRC and PA2S, both of which contain aged charcoal, yielded the largest number of assigned DBC formulae with greater log K_{ow} values (**Figure 6B**). Interestingly, RICEC also yielded a relatively large number of high log K_{ow} DBC formulae. The DBC molecular character of RICEC contradicts what we would expect to observe for fresh charcoal leachates, such as WOODC and PNAC, which yielded lower numbers of identified DBC formulae occupying a lower range of log K_{ow} (**Figure 6B**).

Ultrahigh resolution mass spectrometry is a semi-quantitative method where molecular formulae associated with peaks of higher relative intensity are considered to be more abundant within the sample (Kujawinski et al., 2002). The relative abundance of DBC formula-assigned peaks, categorized according to log K_{ow}, for each soil and char leachate is shown in **Figure 7**. DBC formulae with estimated log K_{ow} values > 5 are not only the most underrepresented with regards to number of assigned molecular formulas, but they are also the least abundant in terms of mass spectral peak intensity. In comparison, DBC formulae with estimated log K_{ow} values < 3 comprised roughly 80% of mass spectral peak intensity. Taken together with the abundance of B5CA and B6CA generated from DBC in soil and char leachates (**Figure 3A**), it seems that the molecular composition of DBC derived from FT-ICR/MS underrepresents this highly condensed aromatic molecular component of the DBC pool. Although, it should be noted that the list of formulas used for K_{ow} modeling (**Table 1**) and to draw subsequent relationships between log K_{ow} and C+H-O (**Figure 2**) included formulas with higher masses and number of carbon atoms >20.

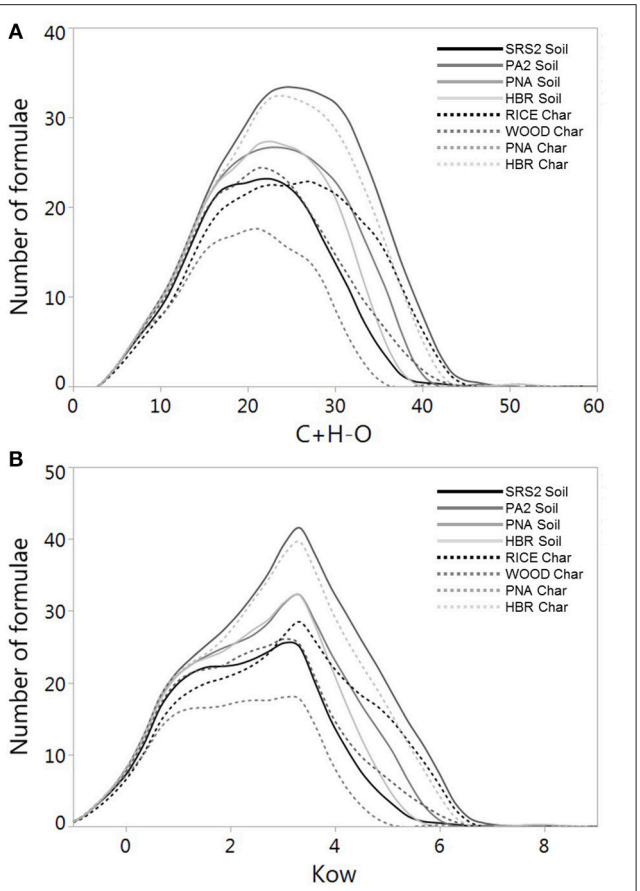

FIGURE 6 | Line plots showing the distribution of **(A)** C+H-O and **(B)** log K_{ow} for DBC formulae identified in soil and char leachates.

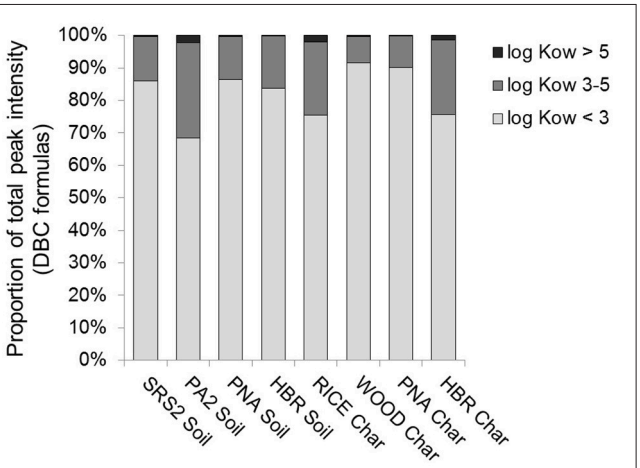

FIGURE 7 | Relative abundance of DBC formula-assigned peaks, as determined from FT-ICR/MS analysis, categorized according to log K_{ow}, for soil and char leachates.

Therefore, the low range of log K_{ow} values for the soil and charcoal leachates is likely, in part, driven by the abundance of DBC formulae with low numbers of carbon. Correlations

between FT-ICR/MS results (total DBC peak intensity, percent DBC peak intensity with log K_{ow} > 5, 3–5, or < 3) and BPCA results (ratios of [B5CA+B6CA]:[B3CA+B4CA] and DBC:DOC) were not significant ($p > 0.1$). We also did not find any significant correlation between DBC concentration and the total number of DBC formulas, or between DBC concentration and the number of DBC formulas in each log K_{ow} class (log K_{ow} < 3, 3–5, and > 5) for the water leachate samples ($R^2 = 0.09$–0.18; $p > 0.3$; $n = 24$). As discussed previously, this is most likely due to the RICE Char sample, which produced significantly more DBC than any other soil or char, thus preventing any meaningful correlations between DBC quantity and quality as described by modeled K_{ow} or mass spectral analysis.

The apparent discrepancy between FT-ICR/MS and BPCA data with regards to DBC quantification and characterization could arise for several reasons. The BPCA method relies on the chromatographic separation and quantification of molecular markers formed from the chemical oxidation of condensed aromatic structures (Dittmar, 2008). Whereas, FT-ICR/MS relies on the soft (non-destructive) ionization of polar, organic molecules comprising the bulk DOM pool, of which DBC is only a part. Although, FT-ICR/MS is semi-quantitative, it is well understood that ionization efficiencies are not equal among different compound classes. Therefore, the mass spectral signal of highly condensed DBC compounds could have been suppressed by more easily ionizable compounds within the bulk DOM pool. Recent research has demonstrated that, based upon FT-ICR/MS analysis and fragmentation of deep sea DOM, a significant degree of structural diversity is contained within assigned molecular formulas (Zark et al., 2017). Although, the exact number of isomers represented by each molecular formula is unknown, Zark et al. (2017) estimate that the number of unique compounds in DOM is at least one order of magnitude greater than the total number of molecular formulas assigned via FT-ICR/MS. Since it is not unreasonable to assume the degree of molecular diversity in soil and charcoal leachates is similar to that of deep sea DOM, we would expect each DBC formula, especially those assigned to higher mass-to-charge ratios, to represent a large number of structural isomers. Therefore, although the expected solubility of individual condensed aromatic structures may be low (based upon calculated K_{ow}), actual bulk concentrations of DBC may be much higher if summed up over all possible isomers associated with each assigned DBC formula. The current study did not exhaustively consider every possible DBC structure. Therefore, we may have underestimated the true solubility of the bulk DBC pool, which may explain, in part, discrepancies between BPCA and mass spectral results. It is also possible that the observed discrepancy results from the overestimation of DBC content via the BPCA method. Previous studies have shown BPCAs to be primarily derived from charred material (Dittmar, 2008; Roth et al., 2012), especially for pyrogenic organic matter formed at high temperatures (Schneider et al., 2010). However, a recent study points to a potentially non-pyrogenic source for some BPCAs (Kappenberg et al., 2016). Since our DBC concentrations are derived from an accumulated total of all BPCAs (including B3CAs and B4CAs, which have been shown to be produced in small quantities from non-pyrogenic organic matter; Kappenberg et al., 2016), the overestimation of DBC is possible. However, since B5CA and B6CA (presumed to be exclusively pyrogenic; Kappenberg et al., 2016), give the most weight in converting BPCA amounts to DBC concentrations (Dittmar, 2008) the slight overestimation of DBC would not significantly change the results or interpretation of the current study. The BPCA and FT-ICR/MS methodologies for detecting DBC across the combustion continuum are fairly well-understood, but not definitively constrained (Masiello, 2004). Although, we assume some portion of their analytical windows to overlap, the observed disconnect between BPCA and FT-ICR/MS data for the soil and char leachates is not unexpected, especially for such a small number of compositionally-varied samples.

Summary and Implications

Identifying the chemical and environmental factors which control the translocation of DBC from the particulate to the dissolved phase and the subsequent stabilization of DBC within the water column is still a largely open question within the pyrogenic carbon research community. The K_{ow} modeling data presented herein suggested that proposed DBC molecular structures presented a large range of solubility, depending on size and degree of condensation, as well as on the degree of oxidation (O-content). However, while 14% of the 90 proposed DBC molecular structures yielded log K_{ow} values indicative of good aqueous solubility, the fraction of the DBC which exhibited limited solubility was still significant (40% has moderate solubility and 46% are considered insoluble). Therefore, we hypothesized that DBC must partition to an intermediate phase, such as DOM, in order to increase apparent solubility of condensed aromatic structures in order to be stabilized in the aqueous phase. However, the results of the current study were unable to provide experimental support for the enhanced mobilization of DBC in the presence of added DOM alone.

The apparent solubility of DBC, which consists of a pool of compounds of diverse molecular size, degree of oxidation, and condensed aromaticity, is likely controlled, in part, by simple aqueous solubility for low log K_{ow} compounds, particularly for less polycondensed and more polar DBC structures. However, controls on the mobilization of larger, highly polycondensed DBC structures are less clear. Stabilization of BC in the dissolved phase may instead be driven by the formation of supramolecular assemblies or micelles, or by association with colloidal fractions and/or microparticulates. While DBC-DOM hydrophobic interactions might play a role in the mobilization process, the formation of molecular assemblies between DBC and DOM components via weak molecular forces and/or interactions with metals may also be important processes to consider. This study highlights the analytical and experimental challenges in unraveling the environmental dynamics of DBC, suggesting that the translocation of soil BC and char to DBC in aquatic systems is controlled by complex biogeochemical processes, whose environmental drivers continue to remain elusive.

AUTHOR CONTRIBUTIONS

YD performed the K_{ow} modeling portion of this study. SW carried out all leaching experiments, performed black carbon and mass spectral analyses. SW drafted the manuscript with significant inputs from YD and RJ, who contributed to the writing and data interpretation.

ACKNOWLEDGMENTS

This work was supported by the National Science Foundation through the Florida Coastal Long Term Ecological Research program (Grant No. DEB-1237517) and the George Barley endowment. The authors thank Dr. Thorsten Dittmar for his insightful feedback on the manuscript and assistance in working up FT-ICR mass spectral data. K. Klaproth is thanked for helping with sample FT-ICR/MS analysis. YD thanks FIU for a DOI Fellowship. The authors thank John Harris for performing the %OC determinations, and Drs. J. Lehmann and J. Campbell for kindly providing the PA2 Soil and HBR Soil sampler, respectively. Support for field logistics for the collection of the PNA samples by Dr. F. Rosario-Ortiz is appreciated. This is Contribution Number 844 from the Southeast Environmental Research Center.

SUPPLEMENTARY MATERIAL

The Supplementary Material for this article can be found online at: http://journal.frontiersin.org/article/10.3389/feart.2017.00075/full#supplementary-material

REFERENCES

Abiven, S., Hengartner, P., Schneider, M. P. W., Singh, N., and Schmidt, M. W. I. (2011). Pyrogenic carbon soluble fraction is larger and more aromatic in aged charcoal than in fresh charcoal. *Soil Biol. Biochem.* 43, 1615–1617. doi: 10.1016/j.soilbio.2011.03.027

Azam, F., and Malfatti, F. (2007). Microbial structuring of marine ecosystems. *Nat. Rev. Microbiol.* 5, 782–791. doi: 10.1038/nrmicro1747

Bird, M. I., Wynn, J. G., Saiz, G., Wurster, C. M., and McBeath, A. (2015). The pyrogenic carbon cycle. *Annu. Rev. Earth Planet. Sci.* 43, 273–298. doi: 10.1146/annurev-earth-060614-105038

Brodowski, S., Rodionov, A., Haumaier, L., Glaser, B., and Amelung, W. (2005). Revised black carbon assessment using benzene polycarboxylic acids. *Org. Geochem.* 36, 1299–1310. doi: 10.1016/j.orggeochem.2005.03.011

Cheng, C.-H., Lehmann, J., Thies, J. E., and Burton, S. D. (2008). Stability of black carbon in soils across a climatic gradient. *J. Geophys. Res.* 113:G02027. doi: 10.1029/2007JG000642

Cheng, C.-H., Lehmann, J., Thies, J. E., Burton, S. D., and Engelhard, M. H. (2006). Oxidation of black carbon by biotic and abiotic processes. *Org. Geochem.* 37, 1477–1488. doi: 10.1016/j.orggeochem.2006.06.022

Chin, Y.-P., Aiken, G. R., and Danielsen, K. M. (1997). Binding of pyrene to aquatic and commercial humic substances: the role of molecular weight and aromaticity. *Environ. Sci. Technol.* 31, 1630–1635. doi: 10.1021/es960404k

Ding, Y., Cawley, K. M., da Cunha, C. N., and Jaffe, R. (2014). Environmental dynamics of dissolved black carbon in wetlands. *Biogeochemistry* 119, 259–273. doi: 10.1007/s10533-014-9964-3

Ding, Y., Yamashita, Y., Dodds, W. K., and Jaffé, R. (2013). Dissolved black carbon in grassland streams: is there an effect of recent fire history? *Chemosphere* 90, 2557–2562. doi: 10.1016/j.chemosphere.2012.10.098

Dittmar, T. (2008). The molecular level determination of black carbon in marine dissolved organic matter. *Org. Geochem.* 39, 396–407. doi: 10.1016/j.orggeochem.2008.01.015

Dittmar, T., de Rezende, C. E., Manecki, M., Niggemann, J., Ovalle, A. R. C., Stubbins, A., et al. (2012). Continuous flux of dissolved organic carbon from a vanished tropical forest biome. *Nat. Geosci.* 5, 618–622. doi: 10.1038/ngeo1541

Dittmar, T., Koch, B., Hertkorn, N., and Kattner, G. (2008). A simple and efficient method for the solid-phase extraction of dissolved organic matter (SPE-DOM) from seawater. *Limnol. Oceanogr. Methods* 6, 230–235. doi: 10.4319/lom.2008.6.230

Dittmar, T., and Koch, B. P. (2006). Thermogenic organic matter dissolved in the abyssal ocean. *Mar. Chem.* 102, 208–217. doi: 10.1016/j.marchem.2006.04.003

Dittmar, T., and Paeng, J. (2009). A heat-induced molecular signature in marine dissolved organic matter. *Nat. Geosci.* 2, 175–179. doi: 10.1038/ngeo440

Durjava, M. K., ter Laak, T. L., Hermens, J. L. M., and Struijs, J. (2007). Distribution of PAHs and PCBs to dissolved organic matter: high distribution coefficients with consequences for environmental fate modeling. *Chemosphere* 67, 990–997. doi: 10.1016/j.chemosphere.2006.10.059

Gauthier, T. D., Seitz, W. R., and Grant, C. L. (1987). Effects of structural and compositional variations of dissolved humic materials on pyrene K_{oc} values. *Environ. Sci. Technol.* 21, 243–248. doi: 10.1021/es00157a003

Goldberg, E. (1985). *Black Carbon in the Environment*. New York, NY: John Wiley and Sons.

Güereña, D. T., Lehmann, J., Walter, T., Enders, A., Neufeldt, H., Odiwour, H., et al. (2015). Terrestrial pyrogenic carbon export to fluvial ecosystems: lessons learned from the White Nile watershed of East Africa. *Glob. Biogeochem. Cycles* 29, 1911–1928. doi: 10.1002/2015GB005095

Hammes, K., Smernik, R. J., Skjemstad, J. O., Herzog, A., Vogt, U. F., and Schmidt, M. W. I. (2006). Synthesis and characterisation of laboratory-charred grass straw (*Oryza sativa*) and chestnut wood (*Castanea sativa*) as reference materials for black carbon quantification. *Org. Geochem.* 37, 1629–1633. doi: 10.1016/j.orggeochem.2006.07.003

Hockaday, W. C., Grannas, A. M., Kim, S., and Hatcher, P. G. (2006). Direct molecular evidence for the degradation and mobility of black carbon in soils from ultrahigh-resolution mass spectral analysis of dissolved organic matter from a fire-impacted forest soil. *Org. Geochem.* 37, 501–510. doi: 10.1016/j.orggeochem.2005.11.003

Hockaday, W. C., Grannas, A. M., Kim, S., and Hatcher, P. G. (2007). The transformation and mobility of charcoal in a fire-impacted watershed. *Geochim. Cosmochim. Acta* 71, 3432–3445. doi: 10.1016/j.gca.2007.02.023

Jaffé, R., Ding, Y., Niggeman, J., Vähätalo, A. V., Stubbins, A., Spencer, R. G. M., et al. (2013). Global charcoal mobilization via dissolution and riverine transport to the oceans. *Science* 340, 345–347. doi: 10.1126/science.1231476

Kaiser, M., Kleber, M., and Berhe, A. A. (2015). How air-drying and rewetting modify soil organic matter characteristics: an assessment to improve data interpretation and inference. *Soil Biol. Biochem.* 80, 324–340. doi: 10.1016/j.soilbio.2014.10.018

Kalbitz, K., Solinger, S., Park, J.-H., Michalzik, B., and Matzner, E. (2000). Controls on the dynamics of dissolved organic matter in soils: a review. *Soil Sci.* 165, 277–304. doi: 10.1097/00010694-200004000-00001

Kappenberg, A., Blasing, M., Lehndorff, E., and Amelung, W. (2016). Black carbon assessment using benzenepolycarboxylic acids: limitations for organic-rich matrices. *Org. Geochem.* 94, 47–51. doi: 10.1016/j.orggeochem.2016.01.009

Karickhoff, S. W. (1981). Semi-empirical estimation of sorption of hydrophobic pollutants on natural sediments and soils. *Chemosphere* 10, 833–846. doi: 10.1016/0045-6535(81)90083-7

Keiluweit, M., and Kleber, M. (2009). Molecular-level interactions in soils and sediments: the role of aromatic π-systems. *Environ. Sci. Technol.* 43, 3421–3429. doi: 10.1021/es8033044

Kleber, M., and Johnson, M. G. (2010). Advances in understanding the molecular structure of soil organic matter: implications for interactions in the environment. *Adv. Agron.* 107, 77–142. doi: 10.1016/S0065-2113(10)06003-7

Knicker, H., Almendros, G., González-Vila, F. J., Martin, F., and Lüdemann, H. D. (1996). ^{13}C- and ^{15}N-NMR spectroscopic examination of the transformation of

organic nitrogen in plant biomass during thermal treatment. *Soil Biol. Biochem.* 28, 1053–1060. doi: 10.1016/0038-0717(96)00078-8

Koch, B. P., and Dittmar, T. (2006). From mass to structure: an aromaticity index for high resolution mass data of natural organic matter. *Rapid Commun. Mass Spectrom.* 20, 926–932. doi: 10.1002/rcm.2386

Koch, B. P., Dittmar, T., Witt, M., and Kattner, G. (2007). Fundamentals of molecular formula assignment to ultrahigh resolution mass data of natural organic matter. *Anal. Chem.* 79, 1758–1763.

Kopinke, F.-D., Georgi, A., Mackenzie, K., and Kumke, M. U. (2002). "Sorption and chemical reactions of polycyclic aromatic hydrocarbons with dissolved refractory organic substances and related model polymers," in *Refractory Organic Substances in the Environment*, eds F. H. Frimmel, G. Abbt-Braun, K. G. Heumann, B. Hock, H.-D. Lüdemann, and M. Spiteller (Weinheim: Wiley), 475–515.

Kothawala, D. N., Roehm, C., Blodau, C., and Moore, T. R. (2012). Selective adsorption of dissolved organic matter to mineral soils. *Geoderma* 189–190, 334–342. doi: 10.1016/j.geoderma.2012.07.001

Kramer, R. W., Kujawinski, E. B., and Hatcher, P. G. (2004). Identification of black carbon derived structures in a volcanic ash soil humic acid by Fourier transform ion cyclotron resonance mass spectrometry. *Environ. Sci. Technol.* 38, 3387–3395. doi: 10.1021/es030124m

Kujawinski, E. B. (2002). Electrospray ionization Fourier transform ion cyclotron resonance mass spectrometry (ESI FT-ICR MS): characterization of complex environmental mixtures. *Environ. Forensics* 3, 207–216. doi: 10.1080/713848382

Kujawinski, E. B., Freitas, M. A., Zang, X., Hatcher, P. G., Green-Church, K. B., and Jones, B. (2002). The application of electrospray ionization mass spectrometry (ESI MS) to the structural characterization of natural organic matter. *Org. Geochem.* 33, 171–180. doi: 10.1016/S0146-6380(01)00149-8

Kuo, D. T. F., Vander Sande, J. B., and Gschwend, P. M. (2013). Characterization of black carbon in geosorbents at the nanometer scale by STEM–EDX elemental mapping. *Org. Geochem.* 56, 81–93. doi: 10.1016/j.orggeochem.2012.12.012

Kuzyakov, Y., Bogomolova, I., and Glaser, B. (2014). Biochar stability in soil: decomposition during eight years and transformation as assessed by compound-specific ^{14}C analysis. *Soil Biol. Biochem.* 70, 229–236. doi: 10.1016/j.soilbio.2013.12.021

Lehmann, J., Solomon, D., Kinyangi, J., Dathe, L., Wirick, S., and Jacobsen, C. (2008). Spatial complexity of soil organic matter forms at nanometer scales. *Nat. Geosci.* 1, 238–242. doi: 10.1038/ngeo155

Lu, R., Sheng, G.-P., Liang, Y., Li, W.-H., Tong, Z.-H., Chen, W., et al. (2013). Characterizing the interactions between polycyclic aromatic hydrocarbons and fulvic acids in water. *Environ. Sci. Pollut. Res.* 20, 2220–2225. doi: 10.1007/s11356-012-1087-6

Masiello, C. A. (2004). New directions in black carbon organic geochemistry. *Mar. Chem.* 92, 201–213. doi: 10.1016/j.marchem.2004.06.043

McBeath, A. V., Smernik, R. J., and Krull, E. S. (2013). A demonstration of the high variability of chars produced from wood in bushfires. *Org. Geochem.* 55, 38–44. doi: 10.1016/j.orggeochem.2012.11.006

Meylan, W. M., and Howard, P. H. (1995). Atom/Fragment contribution method for estimating octanol-water partition coefficients. *J. Pharm. Sci.* 84, 84–92. doi: 10.1002/jps.2600840120

Mitra, S., and Dickhut, R. M. (1999). Three-phase modeling of polycyclic aromatic hydrocarbon association with pore-water-dissolved organic carbon. *Environ. Toxicol. Chem.* 18, 1144–1148. doi: 10.1002/etc.5620180611

Myers-Pigg, A. N., Louchouarn, P., Amon, R. M. W., Prokushkin, A., Pierce, K., and Rubtsov, A. (2015). Labile pyrogenic dissolved organic carbon in major Siberian Arctic rivers: implications for wildfire-stream metabolic linkages. *Geophys. Res. Lett.* 42, 377–385. doi: 10.1002/2014GL062762

Perminova, I. V., Grechishcheva, N. Y., and Petrosyan, V. S. (1999). Relationships between structure and binding affinity of humic substances for polycyclic aromatic hydrocarbons: relevance of molecular descriptors. *Environ. Sci. Technol.* 33, 3781–3787. doi: 10.1021/es990056x

Piccolo, A. (2001). The supramolecular structure of humic substances: a novel understanding of humus chemistry and implications in soil science. *Adv. Agron.* 75, 57–134. doi: 10.1016/S0065-2113(02)75003-7

Reisser, M., Purves, R. S., Schmidt, M. W. I., and Abiven, S. (2016). Pyrogenic carbon in soils: a literature-based inventory and a global estimation of its content in soil organic carbon and stocks. *Front. Earth Sci.* 4:80. doi: 10.3389/feart.2016.00080

Roth, P. J., Lehndorff, E., Brodowski, S., Bornemann, L., Sánchez-García, L., Gustafsson, Ö., et al. (2012). Differentiation of charcoal, soot and diagenetic carbon in soil: method comparison and perspectives. *Org. Geochem.* 46, 66–75. doi: 10.1016/j.orggeochem.2012.01.012

Santín, C., Doerr, S. H., Kane, E. S., Masiello, C. A., Ohlson, M., de la Rosa, J. M., et al. (2015). Towards a global assessment of pyrogenic carbon from vegetation fires. *Global Change Biol.* 22, 76–91. doi: 10.1111/gcb.12985

Schneider, M. P. W., Hilf, M., Vogt, U. F., and Schmidt, M. W. I. (2010). The benzene polycarboxylic acid (BPCA) pattern of wood pyrolyzed between 200°C and 1000°C. *Org. Geochem.* 41, 1082–1088. doi: 10.1016/j.orggeochem.2010.07.001

Schneider, M. P. W., Pyle, L. A., Clark, K. L., Hockaday, W. C., Masiello, C. A., and Schmidt, M. W. I. (2013). Toward a "molecular thermometer" to estimate the charring temperature of wildland charcoals derived from different biomass sources. *Environ. Sci. Technol.* 47, 11490–11495. doi: 10.1021/es401430f

Schneider, M. P. W., Smittenberg, R. H., Dittmar, T., and Schmidt, M. W. I. (2011). Comparison of gas with liquid chromatography for the determination of benzenepolycarboxylic acids as molecular tracers of black carbon. *Org. Geochem.* 42, 275–282. doi: 10.1016/j.orggeochem.2011.01.003

Schwarzenbach, R. P., Gschwend, P. M., and Imboden, D. M. (2003). *Environmental Organic Chemistry: Second Edition*. Hoboken: John Wiley and Sons, Inc.

Seth, R., MacKay, D., and Muncke, J. (1999). Estimating organic carbon partition coefficient and its variability for hydrophobic chemicals. *Environ. Sci. Technol.* 33, 2390–2394. doi: 10.1021/es980893j

Simpson, A. J., Kingery, W. L., Hayes, M. H. B., Spraul, M., Humpfer, E., Dvortsak, P., et al. (2002). Molecular structures and associations of humic substances in the terrestrial environment. *Naturwissenschaften* 89, 84–88. doi: 10.1007/s00114-001-0293-8

Sleighter, R. L., and Hatcher, P. G. (2007). The application of electrospray ionization coupled to ultrahigh resolution mass spectrometry for the molecular characterization of natural organic matter. *J. Mass Spectrom.* 42, 559–574. doi: 10.1002/jms.1221

Stubbins, A., Spencer, R. G. M., Mann, P. J., Holmes, R. M., McClelland, J. W., Niggemann, J., et al. (2015). Utilizing colored dissolved organic matter to derive dissolved black carbon export by arctic rivers. *Front. Earth Sci.* 3:63. doi: 10.3389/feart.2015.00063

Sutton, R., and Sposito, G. (2005). Molecular structure in soil humic substances: the new view. *Environ. Sci. Technol.* 39, 9009–9015. doi: 10.1021/es050778q

Thorn, K. A., Folan, D. W., and MacCarthy, P. (1989). *Characterization of the International Humic Substances Society Standard and Reference Fulvic and Humic Acids by Solution State Carbon-13 (^{13}C) and Hydrogen-1 (^{1}H) Nuclear Magnetic Resonance Spectrometry, U.S. Geological Survey, Water-Resources Investigations Report 89-4196*, Denver, CO, 93.

Tobiszewski, M., and Namiesnik, J. (2012). PAH diagnostic ratios for the identification of pollution emission sources. *Environ. Pollut.* 162, 110–119. doi: 10.1016/j.envpol.2011.10.025

Uhle, M. E., Chin, Y.-P., Aiken, G. R., and McKnight, D. M. (1999). Binding of polychlorinated biphenyls to aquatic humic substances: the role of substrate and sorbate properties on partitioning. *Environ. Sci. Technol.* 33, 2715–2718. doi: 10.1021/es9808447

Wagner, S., Cawley, K. M., Rosario-Ortiz, F., and Jaffé, R. (2015a). In-stream sources and links between particulate and dissolved black carbon following a wildfire. *Biogeochemistry* 124, 145–161. doi: 10.1007/s10533-015-0088-1

Wagner, S., Dittmar, T., and Jaffé, R. (2015b). Molecular characterization of dissolved black nitrogen via electrospray ionization Fourier transform ion cyclotron resonance mass spectrometry. *Org. Geochem.* 79, 21–30. doi: 10.1016/j.orggeochem.2014.12.002

Wagner, S., and Jaffé, R. (2015). Effect of photodegradation on molecular size distribution and quality of dissolved black carbon. *Org. Geochem.* 86, 1–4. doi: 10.1016/j.orggeochem.2015.05.005

Wiedemeier, D. B., Lang, S. Q., Gierga, M., Abiven, S., Bernasconi, S. M., and Früh-Green, G. L. (2016). Characterization, quantification and compound-specific isotopic analysis of pyrogenic carbon using benzene polycarboxylic acids (BPCA). *J. Vis. Exp.* 111:E53922. doi: 10.3791/53922

Yamashita, Y., and Jaffé R. (2008). Characterizing the interactions between trace metals and dissolved organic matter using excitation-emission matrix and parallel factor analysis. *Environ. Sci. Technol.* 42, 7374–7379. doi: 10.1021/es801357h

Zark, M., Christoffers, J., and Dittmar, T. (2017). Molecular properties of deep-sea dissolved organic matter are predictable by the central limit theorem: evidence from tandem FT-ICR-MS. *Mar. Chem.* 191, 9–15. doi: 10.1016/j.marchem.2017.02.005

Zimmerman, A. R. (2010). Abiotic and microbial oxidation of laboratory-produced black carbon (biochar). *Environ. Sci. Technol.* 44, 1295–1301. doi: 10.1021/es903140c

Ziolkowski, L. A., Chamberlin, A. R., Greaves, J., and Druffel, E. R. M. (2011). Quantification of black carbon in marine systems using the benzene polycarboxylic acid method: a mechanistic and yield study. *Limnol. Oceanogr. Methods* 9, 140–149. doi: 10.4319/lom.2011.9.140

Conflict of Interest Statement: The authors declare that the research was conducted in the absence of any commercial or financial relationships that could be construed as a potential conflict of interest.